Discovery of Human-Similar Gene Fusions in Canine Cancers

Ronan Ulvé[1,2,3], Mélanie Rault[1,3], Mathieu Bahin[1,3], Laetitia Lagoutte[1,3], Jérôme Abadie[4], Clotilde De Brito[1,3], Jean-Michel Coindre[5], Nadine Botherel[1,3], Audrey Rousseau[6], Valentin Wucher[1,3], Edouard Cadieu[1,3], Catherine Thieblemont[7], Christophe Hitte[1,3], Laurence Cornevin[8], Florian Cabillic[8], Laura Bachelot[1,3], David Gilot[1,3], Benoit Hennuy[9], Thierry Guillaudeux[3,10], Arnaud Le Goff[2,3], Thomas Derrien[1,3], Benoît Hédan[1,3], and Catherine André[1,3]

Abstract

Canine cancers represent a tremendous natural resource due to their incidence and striking similarities to human cancers, sharing similar clinical and pathologic features as well as oncogenic events, including identical somatic mutations. Considering the importance of gene fusions as driver alterations, we explored their relevance in canine cancers. We focused on three distinct human-comparable canine cancers representing different tissues and embryonic origins. Through RNA-Seq, we discovered similar gene fusions as those found in their human counterparts: *IGK-CCND3* in B-cell lymphoma, *MPB-BRAF* in glioma, and *COL3A1-PDGFB* in dermatofibrosarcoma protuberans-like. We showed not only similar partner genes but also identical breakpoints leading to oncogene overexpression. This study demonstrates similar gene fusion partners and mechanisms in human–dog corresponding tumors and allows for selection of targeted therapies in preclinical and clinical trials with pet dogs prior to human trials, within the framework of personalized medicine. *Cancer Res; 77(21); 5721–7. ©2017 AACR.*

Introduction

During the past decade, pet dogs have arisen as a relevant but underused model for cancer genetics and therapies (1). Although extremely useful for cancer research, rodent models show limitations in their ability to fully reproduce the complexity of spontaneously occurring human tumors (2). As canine tumors address part of these concerns, there is a growing interest in using this "natural cancer resource" in translational cancer research for both

[1]Univ. Rennes 1, CNRS, Institut de Génétique et de Développement de Rennes (IGDR), UMR6290, Rennes, France. [2]BIOTRIAL Pharmacology, Unité de Pharmacologie Préclinique, Rennes, France. [3]UMS 3480 CNRS/US018 INSERM Biosit, Laboratoire Commun Oncotrial, Rennes, France. [4]ONIRIS, AMaROC, Ecole Nationale Vétérinaire, Agroalimentaire et de l'Alimentation Nantes Atlantique, Nantes, France. [5]Institut Bergonié, Bordeaux, France. [6]Département de Pathologie Cellulaire et Tissulaire, CHU, Angers, France. [7]APHP, Hopital Saint-Louis, Hemato-oncologie; Université Paris Diderot, Sorbonne Paris Cité, Paris, France. [8]Laboratoire de Cytogénétique et Biologie Cellulaire, CHU de Rennes, INSERM, INRA, Univ. Rennes 1, Nutrition Metabolisms and Cancer, Rennes, France. [9]GIGA-Genomics, Université de Liège, CHU, 1 Avenue de l'Hopital, Liège, BELGIQUE. [10]ER OSS440 INSERM, Rennes, France.

Note: Supplementary data for this article are available at Cancer Research Online (http://cancerres.aacrjournals.org/).

R. Ulvé and M. Rault contributed equally to and are co-first authors of this article.

B. Hédan and C. André jointly supervised this work.

Corresponding Authors: Benoît Hédan, Université de Rennes 1-CNRS, UMR6290, 2 Avenue Leon Bernard, Rennes 35043, France. Phone: 33-2-2323-4509; Fax: 33-2-2323-4478; E-mail: benoit.hedan@univ-rennes1.fr; and Catherine André, catherine.andre@univ-rennes1.fr

human and dog medicine benefit. Inclusion of pet dogs in preclinical and clinical trials should accelerate the screening of new treatments by reducing the time and cost of evaluating efficacy, pharmacokinetics, and toxicity (3). These advantages have already justified ongoing trials with pet dogs (4).

To use canine cancers as models for the development of new treatments, it is essential to determine human and canine tumors correspondences. The physiopathology of canine tumors presents strong similarities with human tumors in their biological behavior, histopathologic features, and response to treatments (2). Moreover, comparative oncology studies show that some canine and human cancers share similar genetic aberrations, including chromosomal instability, common cytogenetic aberrations, involvement of identical oncogenes or tumor suppressors, and even identical somatic mutations (5). The identification of such driver genetic alterations, both in dogs and humans, is highly informative for the development of dedicated new targeted therapies, such as the development of c-kit inhibitors for canine mast cell disorders (6). Among such driver events, we focused on translocations that generally lead to overexpression of oncogenes. In humans, these recurrent translocations have been described in hematologic disorders, sarcomas, and carcinomas; most of them are specific and even pathognomonic for tumor types and represent precious tools for diagnosis and relevant therapeutic targets (7, 8). Although well described in humans, such translocations in dogs have only been explored and identified by FISH to date, in two canine hematologic tumors: a chronic lymphocytic leukemia with a *BCR-ABL* fusion and a Burkitt lymphoma with a *IGH-MYC* translocation (9).

In the current study, we aim to demonstrate that pet dogs are relevant spontaneous models for human oncology with conserved key gene fusions, not restricted to hematologic disorders

by identifying chimeric transcripts with new and highly resolutive methods (NGS). Thus, we used whole-transcriptome sequencing [RNA sequencing (RNA-Seq)] of cancers with different origins to allow the detection of gene fusions without preconceived candidates. We report here, for the first time, chimeric transcripts in canine cancers reflecting chromosomal translocations that are comparable with human translocations in: a dermatofibrosarcoma protuberans-like (DFSP-like); an oligodendroglioma; and a diffuse large B-cell lymphoma (DLBCL). We then validated these gene fusions on DNA and RNA from the tumors, providing the breakpoint positions at the single-nucleotide resolution. We finally showed that similarly to the orthologous human cancers, these canine cancers not only share identical breakpoints but also overexpression of the targeted oncogenes. These striking molecular similarities between human and canine cancers pave the way for the use of the canine model in targeted therapies for the benefit of both human and dog patients.

Materials and Methods

Samples

Blood and tissue biopsy samples from dogs were collected by a network of veterinarians through the Cani-DNA biobank (http://dog-genetics.genouest.org), which is part of the CRB-Anim infrastructure. The work with dog samples was approved by the CNRS ethical board, France (35-238-13) for UMR6290 and dog owners consented to the use of data for research purposes anonymously. We selected three distinct cancers (lymphomas, sarcomas, and gliomas) representing different tissues (neurologic, subcutis, and hematologic) and different embryonic origins, with known fusions in the human counterpart. The set of samples included three lymphomas (2 DLBCLs and 1 T lymphoma), 2 gliomas, and 1 DFSP-like.

Histologic diagnosis

The diagnosis of the six tumors was reevaluated by dedicated veterinary (J. Abadie) and human pathologists (J.-M. Coindre and A. Rousseau for the DFSP-like and the glioma, respectively). IHC staining was performed using antibodies showing reactivity with the dog's protein according to the manufacturer or to biocompare website: anti-CD34 (Santa Cruz Biotechnology, Ref SC-7045) and anti-PDGFB (Novus Biologicals, Ref NBP1-52533), anti-BRAF (Abbiotec, Ref 251460), anti-CCND3 (Aviva, Ref AVARP03038_P050) for the DFSP-like, the glioma, and DLBCL, respectively. Appropriate negative controls were performed with normal immune serum of rabbit for CCND3 and BRAF, of goat for PDGFRB.

DNA and RNA isolation

The germline DNA from blood, DNA and RNA from tissues were isolated using, respectively, the Blood L, Tissue and RNA II NucleoSpin Kits (Macherey-Nagel) according to the manufacturer's instructions.

RNA-Seq sample preparation and sequencing

RNA-Seq was performed using the GIGA genomics facility. Briefly, Illumina Truseq RNA Sample Preparation Kit V2 was used to prepare libraries from 1 μg of total RNA with an RNA integrity number greater that 7.3 (Agilent Technologies). Poly-A RNAs were purified with polyT-coated magnetic beads and chemically fragmented to a median size of 200 nucleotides.

These were used as a template for first-strand synthesis in the presence of random hexamers and second-strand synthesis afterward. Next, double stranded cDNA ends were end-blunted and adenylated at 3′OH extremities before ligation to adaptors containing the indexes. Finally, the adapter-ligated library fragments were enriched by PCR following Illumina's protocol and purified with Ampure XP magnetic beads (Agencourt). Final libraries were validated on a Bioanalyser DNA 1000 chip (Agilent Technologies) and quantified by qPCR with the KAPA Library Quantification Kit (Kapa Biosystems). Sequencing was performed on an Illumina HiSeq 2000 instrument using the PE 2 × 100 cycles protocol.

Identification of fusion transcripts

Candidate gene fusion transcripts were identified with CRAC and chimCT softwares (http://cractools.gforge.inria.fr/) using the CanFam3 canine genome reference. Fusion transcripts were manually filtered by discarding transcripts with less than five reads spanning the fusion junction and three reads encompassing the two fusion transcripts, as well as transcripts involving paralogous genes or pseudogenes, transcripts identified as read-through, transcripts with no Ensembl annotation (Supplementary Table S1).

RT-PCR

Reverse transcription was performed on 1 μg of total RNA from tumor or healthy tissue using the High-Capacity cDNA Reverse Transcription Kit (Applied Biosystems) according to the manufacturer's instructions.

Validation of the fused transcript

PCR amplifications were performed on cDNA samples diluted 1:40 using the Type-it Microsatellite PCR Kit (Qiagen) with dedicated primers (Supplementary Table S2). PCR products were sequenced with a 370 ABI sequencer using the BigDye Terminator v3.1 Cycle Sequencing Kit (Applied Biosystems). The presence of fusion transcripts was assessed by alignment of sequences on the CanFam 3 reference dog sequence (https://genome.ucsc.edu/).

Breakpoint mapping on genomic DNA

PCR amplifications were performed on DNA to validate fusion transcripts. Primers specific for each breakpoint (Supplementary Table S2) were designed on CanFam3 to span the candidate introns flanking the identified exons in the chimeric transcripts. All combinations between forward and reverse primers from translocated chromosomes were tested. The large regions of about 1 kb were amplified from 10 ng/μL diluted DNA samples using the Phusion Hot Start II DNA Polymerase Kit (Thermo Fisher Scientific).

Exon expression analysis RT-PCR

qRT-PCR was performed on cDNA samples diluted 1:20 with the SYBR Green PCR Master Mix on the 7900HT Fast Real-Time PCR System (Applied Biosystems) using standard procedures. Each PCR was carried out in triplicate. Relative amounts of the transcript were determined using the $\Delta\Delta C_t$ method. Canine *HPRT* gene (ENSCAFG00000018870) for the lymphoma and the DFSP-like, and *TBP* gene (ENSCAFG00000004119) for the glioma, were used as housekeeping genes. The mRNA levels in each tumor were calculated as a fold increase compared with at least 6 different

healthy tissue mRNA controls: 6 healthy skin samples, 8 healthy cortex samples, 6 healthy lymph nodes for the fibrosarcoma, glioma, and lymphoma, respectively.

Western blot analysis

Cellular protein extracts were prepared using a cell lysis buffer containing 20 mmol/L Tris-HCl pH 7.5, 150 mmol/L NaCl, 1 mmol/L EDTA, 1 mmol/L EGTA and supplemented with 1 mmol/L PMSF, 1× EDTA-free cocktail protease inhibitor (Roche Diagnostics), 30 mmol/L sodium fluoride, 40 mmol/L glycero phosphate, 1 mmol/L sodium orthovanadate, and 0.5% Triton X-100. Protein concentrations were determined by the BCA protein assay (Sigma-Aldrich) using BSA as a standard.

Protein samples were denatured for 10 minute at 95°C, and equal amounts of cell proteins (20 µg) were subjected to 10% SDS-PAGE and transferred onto nitrocellulose membranes (Amersham - GEH Life). Membranes were probed with suitable antibodies. The primary antibodies were: anti-BRAF (Ref 251460, 1:5000, Abbiotec) and anti–β-actin (BA3R, 1:5,000, Millipore). Horseradish peroxidase–conjugated secondary antibodies were purchased from Jackson ImmunoResearch. Signals were detected using the LAS-4000 Imager (Fuji Photo Film). siRNAs were purchased from IDT DNA:

siBRAF1: 5′- CAUGAAGACCUCACAGUAAAAAUAG-3′,
siBRAF2 5′- GACCAAAUUUGAGAUGAUAAAGCTT-3′,
siCTR (NC1) 5′-CGUUAAUCGCGUAUAAUACGCGUAT-3′

Two siRNAs targeting *BRAF* were designed to target two distinct regions of *BRAF* (nucleotides 1717-1740, 1599-1623, respectively, for ENSCAFT00000006305) and ordered to IDT DNA. siRNAs were transfected into human melanoma cells 501Mel or into a canine oral melanoma cell line, kindly provided by Dr. D. Tierny (Oncovet-Vetotech, Villeneuve d'Ascq, France), using Lipofectamine RNAiMAX (Life Technologies) following the manufacturer's instructions. Three days later, BRAF expression levels were analyzed by Western blotting experiments.

FISH experiments

MBP-BRAF fusion tests were performed on 4-µm sections of formalin-fixed paraffin-embedded tissue blocks using the bacterial artificial chromosome (BAC) clones 42G22- 97M23 and 160H02-360E1 (http://bacpacresources.org/library.php?id=253). These BAC clones were labeled with green-dUTP (Abbott Molecular) and Cy3-dCTP (Amersham Biosciences) and hybridized proximal

to *MBP* and distal to the *BRAF* breakpoint regions, respectively. Slides were analyzed by an experienced cytogeneticist (F. Cabillic), using a fluorescence microscope (Axioskop2, Axio Imager Z2, Zeiss) and Isis imaging software (Metasystems). Per case, at least 100 nonoverlapping tumor nuclei were examined.

Statistical analysis

All statistical tests were performed with the R software.

Results and Discussion

Previous cytogenetic studies have underlined the importance of gene fusions in hematologic disorders and sarcoma in humans (8). To investigate gene fusions in canine cancers, we analyzed six tumors belonging to three distinct cancers, representing different tissues (neurologic, subcutis, and hematologic) and embryonic origins, and for which the human corresponding tumors are known to involve key gene fusions. We performed RNA-Seq, using dedicated softwares, followed by classical filters and manual curation to exclude false-positive chimeras; we finally identified 3 gene fusions in 3 of the 6 tumors (Table 1; Supplementary Table S1).

1-A *COL3A1-PDGFB* fusion in a canine DFSP-like

In human DFSP, the translocation t(17;22) leading to the fusion of the collagen type 1 alpha 1 (*COL1A1*) and platelet-derived growth factor B chain (*PDGFB*) genes is considered as pathognomonic of DFSP (10). Thus, we analyzed a canine DFSP-like case (Supplementary Fig. S1) and found a chimeric transcript resulting from the fusion between the collagen type 3 alpha 1 (*COL3A1*) and the *PDGFB* genes. As *COL3A1* and *COL1A1* are paralogous genes, we anticipated that this canine translocation is similar to the human one. Indeed, as in humans, the breakpoint in *PDGFB* is localized in intron 1 (Fig. 1A); moreover, the fusion validation on the cDNA and the genomic DNA of this tumor (Fig. 1B–D) shows a conserved reading frame between the first *COL3A1* exons and the exon 2 of *PDGFB*. Similar to the situation in human DFSP (11), we hypothesized that this translocation, placing *PDGFB* under the regulation of the *COL3A1* promoter, induces the overexpression of *PDGFB* in the canine DFSP-like tumor. This is confirmed by the expression levels of exons retained in the chimeric transcript, which are increased on average 9.6-fold in comparison with healthy tissues ($P < 0.001$, one-tailed Wilcoxon test; Fig. 1E). Moreover, PDGFB protein is detectable in the tumor

Table 1. Fusions identified by RNA-Seq in the canine tumors

Canine tumors	Gene 1	Gene 2	Chromosomal positions	Number of reads spanning the fusion junction	Number of paired reads encompassing the two fusion transcripts
Dermatofibrosarcoma protuberans–like (DFSP-like)	*PDGFB*	*COL3A1*	CFA10: 25,807,321 (strand −)/CFA36: 30,511,682 (strand −)	181	491
Anaplastic oligodendroglioma	*MBP*	*BRAF*	CFA1: 2,919,660 (strand +)/CFA16: 8,270,092 (strand +) CFA1: 2,923,624 (strand +)/CFA16: 8,264,593 (strand +) CFA16: 8,262,734 (strand +)/CFA1: 2,926,747 (strand +) CFA16: 8,270,092 (strand +)/CFA1: 2,919,740 (strand +)	115	344
Diffuse large B-cell lymphoma (DLBCL)	*CCND3*	*IGK*	CFA12: 10,687,874 (strand −)/CFA17: 37,727,274 (strand +) CFA12: 10,687,876 (strand −)/CFA17: 37,709,802 (strand +)	15	10

NOTE: Partner genes and chromosomal positions are indicated for the three tumors, with the number of reads spanning the fusion junction and encompassing the two fusion transcripts.

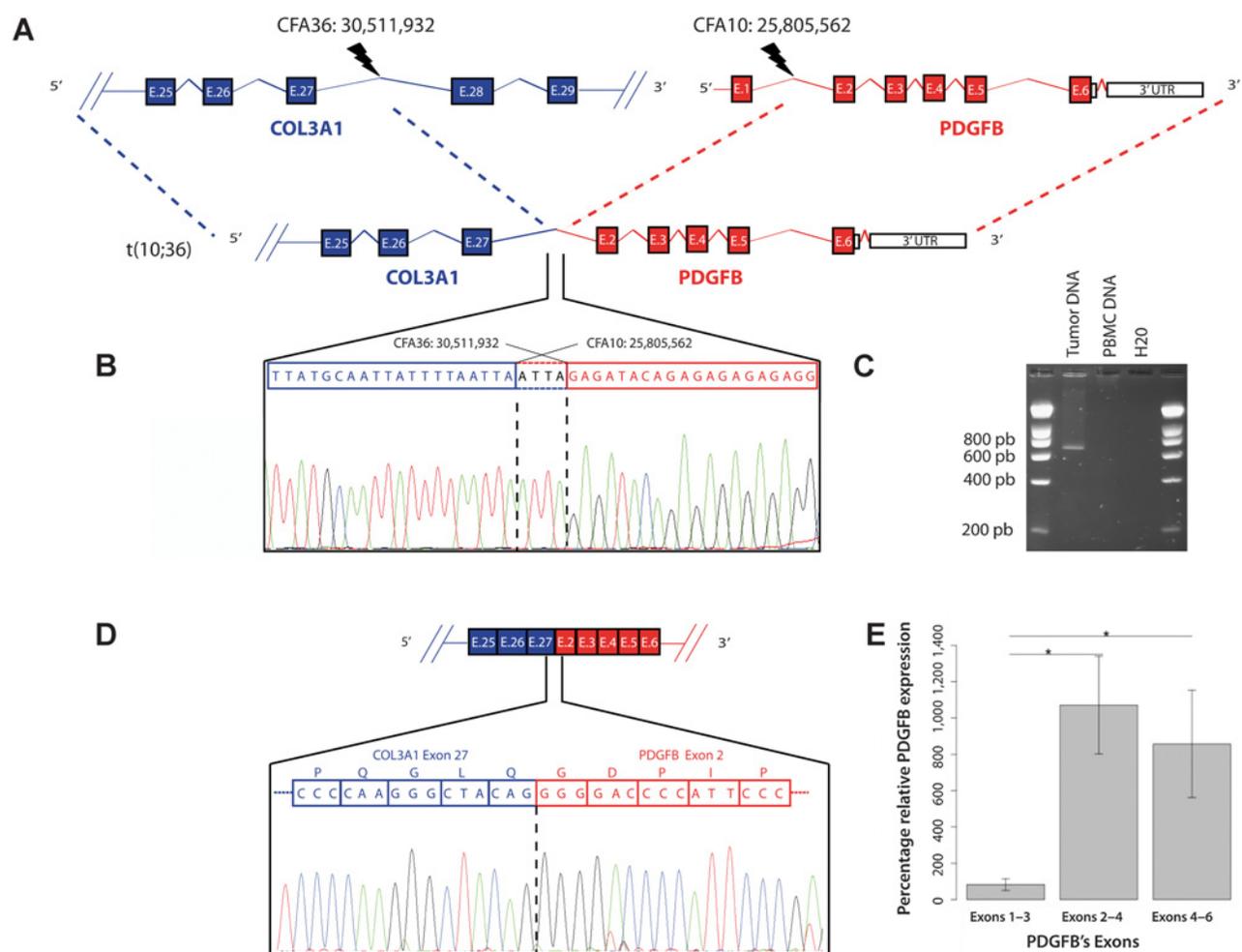Abbreviation: CFA, *Canis familiaris* autosome.

Figure 1.
Characterization of the *COL3A1-PDGFB* fusion. **A,** Scheme of the t(10;36). Exons of *COL3A1* (ENSCAFT00000047312) and *PDGFB* (ENSCAFT00000002101) are depicted as well as the breakpoint positions on CFA36 (blue) and CFA10 (red), indicated with ⚡. CFA, *Canis familiaris* autosome. **B,** Sequence of the breakpoint on genomic DNA. The three nucleotides flanking the dotted line map to both chromosomes. **C,** Electrophoresis of PCR products detects the translocation in tumor but not in the germinal blood DNA of this case. **D,** Scheme of the transcription resulting from the t(10;36). The sequence of the tumor cDNA reveals the expression of one fusion transcript involving exon 27 of *COL3A1* and exon 2 of *PDGFB*. **E,** Relative expression levels of *PDGFB* exons in the tumor in comparison with 6 healthy skin samples (*, $P < 0.05$, one-tailed paired-samples Wilcoxon test). Expression levels of exons 2 to 6 show overexpression of *PDGFB* exons retained in the chimeric transcript. The *PDGFB* wild-type transcript expression, represented by expression levels of exons 1–3, shows no significant difference in the tumor in comparison with an expected value of 100% ($P = 0.31$, two-tailed one-sample Wilcoxon test). These results indicate that the overexpression of *PDGFB* exons in the chimeric transcript is the consequence of the fusion.

by immunostaining (Supplementary Fig. S1). Complementary to this, the alignment of canine and human PDGFB protein sequences (Supplementary Fig. S2) shows the conservation of the two proteolytic cleavage sites in the canine PDGFB and in the putative chimeric protein resulting from *COL3A1/PDGFB* fusion. Under these conditions, the canine *COL3A1/PDGFB* should produce a chimeric precursor protein, transformed into a mature growth factor after proteolysis and forming an autocrine loop, as for the human *COL1A1/PDGFB* fusion (11). As the chimeric protein COL1A1/PDGFB is targeted by imatinib for human DFSP (7, 10), regarding the genetic and biological similarities between human DFSP and canine DFSP-like, we predict similarities in treatment responses. Finally, we propose the *COL3A1* gene as a new candidate partner gene for human DFSP, like the recently discovered *COL1A2* (12).

2-A *MBP-BRAF* fusion in a canine glioma

Human gliomas are a heterogeneous group of tumors of the central nervous system with *BRAF* alterations (somatic mutations or fusions) described almost in all subgroups (13). Therefore, we analyzed two canine grade 3 anaplastic oligodendrogliomas (WHO classification; Supplementary Fig. S3). In one of them, we identified a relevant chimeric transcript resulting from the fusion between the Myelin Basic Protein (*MBP*) and the B-Raf proto-oncogene (*BRAF*) genes. Like in human gliomas with breakpoints localized between *BRAF* intron 8 and 10 (14), the breakpoint of *BRAF* in this canine glioma is within intron 7, orthologous to human *BRAF* intron 8 (Fig. 2A). This fusion was validated on the cDNA and the genomic DNA of this tumor (Fig. 2B–D). The reading frame is conserved between the first *MBP* exons and the last exons of
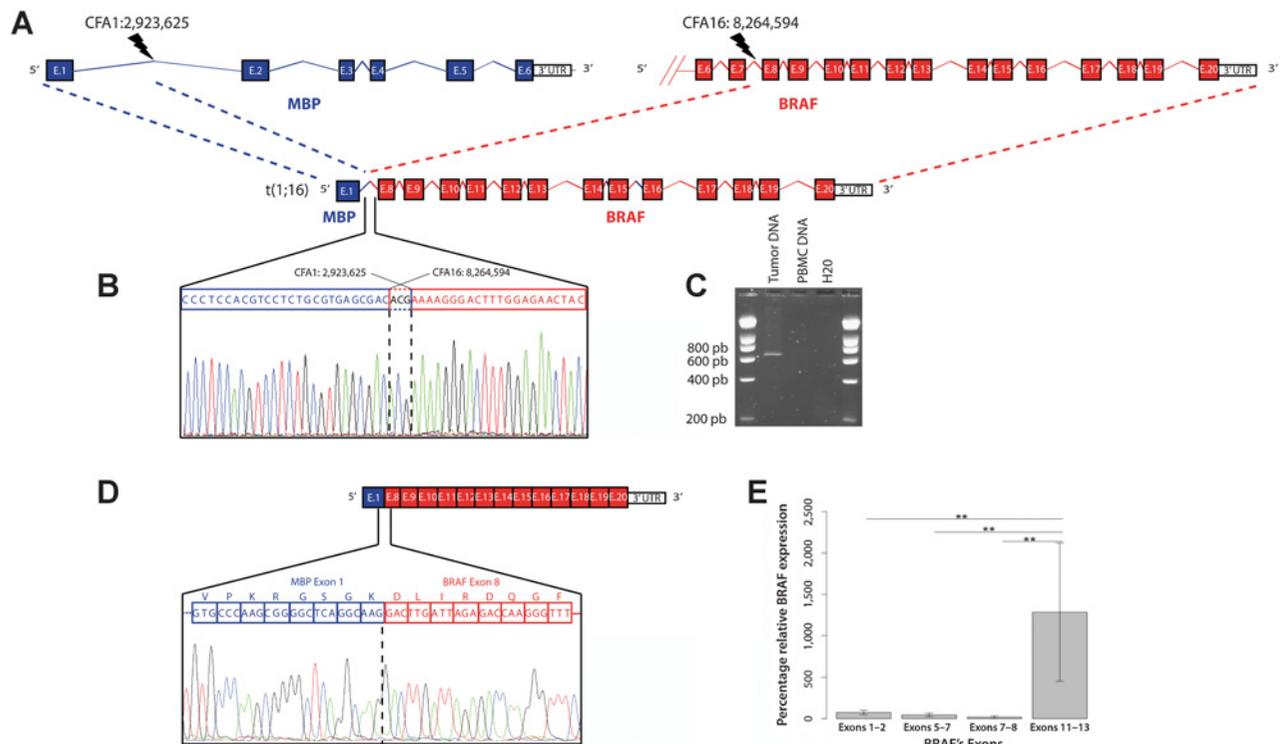
Figure 2.
Characterization of the *MBP-BRAF* fusion. **A,** Scheme of the t(1;16) translocation. Exons of *MBP* (ENSCAFT00000000024) and *BRAF* (ENSCAFT00000006305) are depicted as well the breakpoint positions on CFA1 (blue) and CFA16 (red), indicated with ⚡. CFA, *Canis familiaris* autosome. **B,** Sequence of the breakpoint on genomic DNA. The three nucleotides flanking the dotted line map to both chromosomes. **C,** Electrophoresis of the PCR product detecting the translocation in tumor DNA but not on germinal blood DNA of this case. **D,** Scheme of the transcript resulting from the t(1;16) translocation. The sequence of the tumor cDNA reveals the expression of one fusion transcript involving the exon 1 of *MBP* with exon 8 of *BRAF*. **E,** The histogram shows the relative expression levels of *BRAF* exons in the tumor in comparison with 8 healthy brain samples. The fusion induced overexpression of the retained exons 11–13 on average 12.8-fold ($P \leq 0.01$, one-tailed Wilcoxon test) in comparison with healthy canine brain tissues. The retained exons were overexpressed in comparison with exons localized in 5' of the breakpoint (**, $P \leq 0.01$, two-tailed paired two-sample t test). Expression levels of exons 7–8, flanking the breakpoint, showed that the *BRAF* wild-type transcript is significantly underexpressed in the tumor ($P \leq 0.01$, one-tailed Wilcoxon test). These results showed that the overexpression of BRAF exons retained in the chimeric transcript is linked to the fusion.

BRAF. As the *MBP* promoter is strongly active in glioma cells (15), we anticipated that this translocation could also induce *BRAF* overexpression. We confirmed this hypothesis by measuring the expression levels of exons retained in the chimeric transcript; there was an average 12.8-fold increase in comparison with healthy tissues ($P = 0.0039$, one-tailed Wilcoxon test; Fig. 2E). Moreover, BRAF protein is detectable in the tumor by immunostaining, and a fused protein is detectable in the tumor sample by Western blot analysis (Supplementary Fig. S3). As the alignments of the canine and human BRAF protein sequences showed that the canine chimeric protein has lost its N-terminal autoinhibitory domain (Supplementary Fig. S4), this alteration should induce a constitutive BRAF kinase activity as shown in human cancers (16). In human gliomas, *BRAF* is mainly fused with *KIAA1549*, but other partners have been described (14); while most of these fusions are found in astrocytomas, they are also reported in oligodendrogliomas (17). We propose *MBP* as a new candidate partner for *BRAF* fusions in human gliomas. For these human tumors, with limited therapeutic options, *BRAF* alterations offer new therapeutic strategies and clinical trials are ongoing (16). In this context, spontaneous canine glioma with *BRAF* fusions

provides a unique model to develop new and more efficient treatments.

3-An *IGK-CCND3* fusion in a canine B-cell lymphoma

In human lymphomas, alterations during the natural recombination process of immunoglobulin genes lead commonly to fusions with oncogenes associated with their overexpression. Thus we analyzed three canine lymphomas (two DLBCLs, and one T-cell lymphoma) and found one aberrant transcript revealing a fusion between the Immunoglobulin light chain kappa locus (*IGK*) with Cyclin-D3 (*CCND3*) in one DLBCL sample (Table 1; Fig. 3A). This fusion was validated on the cDNA and the genomic DNA of this tumor (Fig. 3B–D). Such translocations involving *CCND3* and immunoglobulin genes have already been described in human B-cell malignancies, including DLBCL, which could explain the overexpression of *CCND3* found in 10% of human DLBCL (18). Thus, we anticipated that the canine translocation also induces the overexpression of *CCND3*. This is supported by the fact that *CCND3* is overexpressed in canine DLBCL (Fig. 3E), and the CCND3 protein is easily detectable by IHC in the canine DLBCL (Supplementary Fig. S5). Although *IGK-CCND3* fusion was
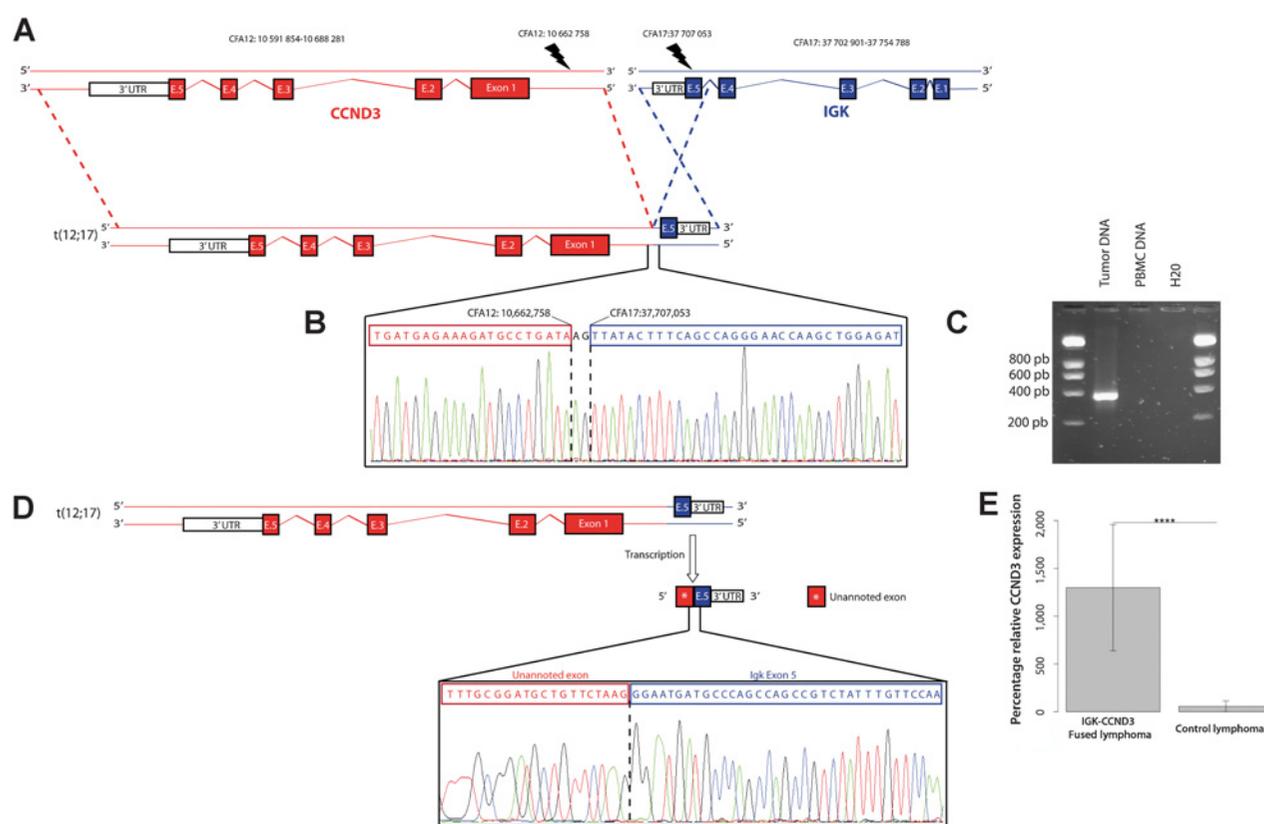
Figure 3.
Characterization of the *IGK-CCND3* translocation in a canine DLBCL. **A,** Schematic representation of the t(12;17) translocation. Exons of *CCND3* (ENSCAFT00000002538) and *IGK* (ENSCAFT00000011790) are depicted as well as the breakpoint positions on CFA12 (red) and CFA17 (blue), indicated with ⚡. CFA, *Canis familiaris* autosome. **B,** Sequence of the breakpoint on genomic DNA. **C,** Electrophoresis of the PCR product detecting the translocation in the tumor DNA but not in the germinal blood DNA of this case. **D,** Scheme of the transcription resulting from t(12;17) translocation. The sequence of the tumor cDNA reveals the expression of one fusion transcript involving a not yet annotated exon of CFA12 with exon 5 of *IGK*. **E,** qRT-PCR experiments show the overexpression of the *CCND3* mRNA transcript in the tumor, on average 13-fold ($P < 0.05$, one-tailed one-sample Wilcoxon test) and 22-fold (****, $P < 10^{-4}$, one-tailed two-sample Wilcoxon test), as compared with 6 healthy lymph nodes and 6 other DLBCLs, respectively.

not identified in human lymphomas, overexpression of *CCND3* driven by *IG*-mediated translocations is expected and searched in cases showing breakapart probes for *CCND3*. Moreover, fusions involving *IGK* and other cyclins, of which, *CCND2* has already been detected (19). In addition, the overexpression of *CCND3* in human DLBCL is a prognostic factor associated with poor clinical outcome (20). Thus, canine lymphomas with fusions involving cyclin D could be used for clinical trials targeting cyclins.

Conclusion

Our work reveals similar fusions in corresponding cancers between dogs and humans and identifies for the first time chimeric transcripts involving the same fused oncogenes with similar rearrangements leading to malignancy. The identification of these three fused transcripts in three different tumors supports the existence of other fused transcripts in other subtypes of canine cancers, similar to what is found in humans. With NGS methods, which are revolutionizing the identification of gene fusions without preconceived idea of partner genes, such canine models will benefit the scientific community, allowing development of new targeted therapies. In the context of the "One Health" concept,

such results of comparative oncology lead us to anticipate that human and veterinary medicine will benefit from clinical trials that include pet dogs as patients.

Disclosure of Potential Conflicts of Interest

T. Guillaudeux is a consultant/advisory board member for Biotrial. No potential conflicts of interest were disclosed by the other authors.

Authors' Contributions

Conception and design: R. Ulvé, M. Rault, T. Guillaudeux, A. Le Goff, B. Hédan, C. André

Development of methodology: M. Rault, E. Cadieu

Acquisition of data (provided animals, acquired and managed patients, provided facilities, etc.): R. Ulvé, M. Rault, L. Lagoutte, J. Abadie, C. De Brito, N. Botherel, A. Rousseau, L. Cornevin, F. Cabillic, L. Bachelot, D. Gilot, B. Hennuy, B. Hédan

Analysis and interpretation of data (e.g., statistical analysis, biostatistics, computational analysis): R. Ulvé, M. Rault, M. Bahin, J. Abadie, J.-M. Coindre, V. Wucher, C. Hitte, F. Cabillic, D. Gilot, T. Guillaudeux, T. Derrien, B. Hédan, C. André

Writing, review, and/or revision of the manuscript: R. Ulvé, M. Rault, J. Abadie, J.-M. Coindre, A. Rousseau, C. Thieblemont, T. Guillaudeux, T. Derrien, B. Hédan, C. André

References

1. Paoloni M, Khanna C. Translation of new cancer treatments from pet dogs to humans. Nat Rev Cancer 2008;8:147–56.
2. Rowell JL, McCarthy DO, Alvarez CE. Dog models of naturally occurring cancer. Trends Mol Med 2011;17:380–8.
3. Paoloni M, Webb C, Mazcko C, Cherba D, Hendricks W, Lana S, et al. Prospective molecular profiling of canine cancers provides a clinically relevant comparative model for evaluating personalized medicine (PMed) trials. PLoS One 2014;9:e90028.
4. LeBlanc AK, Breen M, Choyke P, Dewhirst M, Fan TM, Gustafson DL, et al. Perspectives from man's best friend: National Academy of Medicine's Workshop on Comparative Oncology. Sci Transl Med 2016;8:324ps5.
5. Schiffman JD, Breen M. Comparative oncology: what dogs and other species can teach us about humans with cancer. Philos Trans R Soc Lond B Biol Sci 2015;370:pii:20140231.
6. Ranieri G, Marech I, Pantaleo M, Piccinno M, Roncetti M, Mutinati M, et al. In vivo model for mastocytosis: a comparative review. Crit Rev Oncol Hematol 2015;93:159–69.
7. Greco A, Roccato E, Miranda A, Cleris L, Formelli F, Pierotti MA. Growth-inhibitory effect of STI571 on cells transformed by the COL1A1/PDGFB rearrangement. Int J Cancer 2001;92:354–60.
8. Mertens F, Johansson B, Fioretos T, Mitelman F. The emerging complexity of gene fusions in cancer. Nat Rev Cancer 2015;15:371–81.
9. Breen M, Modiano JF. Evolutionarily conserved cytogenetic changes in hematological malignancies of dogs and humans–man and his best friend share more than companionship. Chromosome Res 2008;16:145–54.
10. Dhir M, Crockett DG, Stevens TM, Silberstein PT, Hunter WJ, Foster JM. Neoadjuvant treatment of Dermatofibrosarcoma Protuberans of pancreas with Imatinib: case report and systematic review of literature. Clin Sarcoma Res 2014;4:8.
11. Simon MP, Pedeutour F, Sirvent N, Grosgeorge J, Minoletti F, Coindre JM, et al. Deregulation of the platelet-derived growth factor B-chain gene via fusion with collagen gene COL1A1 in dermatofibrosarcoma protuberans and giant-cell fibroblastoma. Nat Genet 1997;15:95–8.
12. Nakamura I, Kariya Y, Okada E, Yasuda M, Matori S, Ishikawa O, et al. A novel chromosomal translocation associated with COL1A2-PDGFB gene fusion in dermatofibrosarcoma protuberans: PDGF expression as a new diagnostic tool. JAMA Dermatol 2015;151:1330–7.
13. Penman CL, Faulkner C, Lewis SP, Kurian KM. Current understanding of BRAF alterations in diagnosis, prognosis, and therapeutic targeting in pediatric low-grade gliomas. Front Oncol 2015;5:54.
14. Forbes SA, Beare D, Gunasekaran P, Leung K, Bindal N, Boutselakis H, et al. COSMIC: exploring the world's knowledge of somatic mutations in human cancer. Nucleic Acids Res 2015;43:D805–11.
15. Miyao Y, Shimizu K, Tamura M, Akita H, Ikeda K, Mabuchi E, et al. Usefulness of a mouse myelin basic protein promoter for gene therapy of malignant glioma: myelin basic protein promoter is strongly active in human malignant glioma cells. Jpn J Cancer Res 1997;88:678–86.
16. Lo H-W. Targeting Ras-RAF-ERK and its interactive pathways as a novel therapy for malignant gliomas. Curr Cancer Drug Targets 2010;10:840–8.
17. Badiali M, Gleize V, Paris S, Moi L, Elhouadani S, Arcella A, et al. KIAA1549-BRAF fusions and IDH mutations can coexist in diffuse gliomas of adults. Brain Pathol 2012;22:841–7.
18. Sonoki T, Harder L, Horsman DE, Karran L, Taniguchi I, Willis TG, et al. Cyclin D3 is a target gene of t(6;14)(p21.1;q32.3) of mature B-cell malignancies. Blood 2001;98:2837–44.
19. Wlodarska I, Dierickx D, Vanhentenrijk V, Van Roosbroeck K, Pospisilova H, Minnei F, et al. Translocations targeting CCND2, CCND3, and MYCN do occur in t(11;14)-negative mantle cell lymphomas. Blood 2008;111:5683–90.
20. Filipits M, Jaeger U, Pohl G, Stranzl T, Simonitsch I, Kaider A, et al. Cyclin D3 is a predictive and prognostic factor in diffuse large B-cell lymphoma. Clin Cancer Res 2002;8:729–33.